

# DYNAMIC EFFECTS IN A RESONANT MICRO HEAT ENGINE

H. Bardaweel<sup>1</sup>, M. Anderson<sup>2</sup>, R. Richards<sup>1</sup>, C. Richards<sup>1</sup>

<sup>1</sup>School of Mechanical & Materials Engineering, Washington State University, Pullman, WA USA

<sup>2</sup>Department of Mechanical Engineering, University of Idaho, Moscow, ID USA

**Abstract:** In this paper the behavior of a dynamic micro heat engine is presented. In particular the coupling between the engine dynamics and engine performance is investigated. A lumped parameter model is developed to study dynamic effects. Experiments are performed to validate the model. The model is then used to identify engine parameters that lead to high engine efficiency. The effects of heat pulse duration and frequency; as well as, the relationship between damping and mass on engine efficiency are investigated.

**Key Words:** MEMS power, micro heat engine

## 1. INTRODUCTION

Because macro-scale heat engines have achieved both high power densities and high conversion efficiencies there have been many attempts over the last decade to produce a MEMS heat engine based on Otto, Brayton and Rankine cycles [1-3]. Realizing micro-scale versions of macroscale machinery has proven challenging, although steady progress has been made toward batch fabrication of silicon-based turbomachinery.

Our group has focused on developing a micro heat engine based on flexing components [4]. The engine consists of four major components; a thermal switch to control heat addition and rejection, an evaporator, an engine cavity to convert the heat to mechanical work, and a generator to convert the mechanical work produced by the engine to electrical work. In previous work we have shown the engine produces net mechanical power when operated at low frequency from a constant heat source at 60 C° [5]. At these conditions, although net power was produced, the efficiency was very low, less than 1%.

One route to higher efficiency is to operate at resonance. For example, the generator, the mechanical to electrical work conversion device, is an electromechanical oscillator. For electro-mechanical oscillators resonant operation is desirable for maximum conversion efficiency. In addition, flexing components rather than rotating machinery are used for expansion the coupling between dynamics, thermodynamics and heat

transfer begins to play a major role in the engine performance. The engine may be viewed as a system consisting of several subsystems; namely, the expander/compressor, evaporator, and cavity. Each component or subsystem has a set of thermal and mechanical properties that are optimal. The performance of the engine, or system, is a result of the complex interactions of these properties. Understanding the trade-offs in the design space that control engine power and efficiency entails dealing with all of these issues together simultaneously.

Viewing the engine as a system with an input, heat, and a response, work, allows us to use a transfer function approach for analysis of engine performance. An FFT analysis of experimental parameters allows us to deconstruct the spectral behavior of the engine.

In addition, we have developed a linear lumped parameter model of the engine to characterize the dynamic operation. This will allow a transfer function approach to analysis. As in the experiments, heat is the input and the expander motion is the output. An FFT analysis of experimental parameters allows for a direct comparison to the model output. In this manner the model and experiments may be used to identify key design parameters for engine performance.

## 2. APPROACH

### 2.1 Experiment

The basic engine, shown in Fig. 1, consists of a

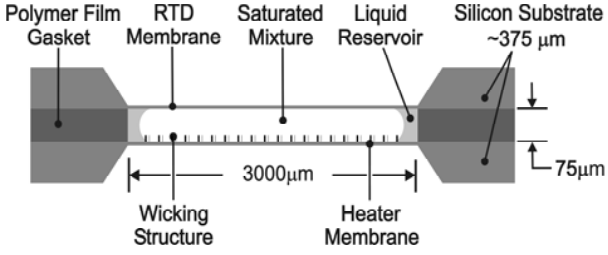


Fig. 1. Micro heat engine schematic.

cavity filled with a two-phase fluid bounded by top and bottom membranes. The bottom membrane acts as an evaporator. A capillary wick fabricated on the bottom membrane controls the layer of liquid-phase working fluid on the evaporator. The top membrane acts as an expander. The thermal switch controls the timing and duration of the heat addition and heat rejection. Mechanical power is produced as the top membrane alternately expands and compresses the working fluid. Mechanical power may be converted into electrical power through the use of a thin-film piezoelectric membrane generator fabricated on the top membrane. Fabrication details are provided in [4,5].

For these experiments the thermal switch was replaced with a resistance heater so that the input heat pulse could be accurately characterized for model validation. A periodic voltage  $V_h(t)$  with period  $T_p$  was supplied to the resistance heater. The motion of the upper membrane was measured with a laser vibrometer. A linear transfer function analysis was used to interpret the data collected from the experiment. The heat rate  $q(t)$  delivered to the engine was the input and the velocity of the upper membrane  $u(t)$  was the output.

## 2.2 Lumped parameter model & analysis

A schematic diagram of the idealized engine is shown in Figure 2. The expander/compressor is modeled as a moveable rigid diaphragm which is constrained by a spring of stiffness  $s$  and two dampers with coefficients  $b_f$  and  $b$  respectively. A moveable rigid evaporator provides the lower boundary.

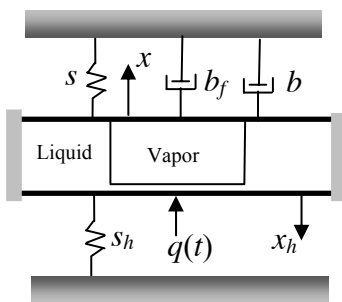


Fig. 2. Model engine.

The motion of the upper diaphragm and evaporator are measured by the displacements  $x$  and  $x_h$  respectively. The engine is powered by a periodic alternating heat flux  $q(t)$  applied to the evaporator component. The cavity is of diameter  $2r_o$ , and contains a saturated-vapor bubble of diameter  $2r_i$  and liquid in the annulus.

A lumped-parameter mathematical model of the engine was developed by applying conservation laws to the vapor bubble and liquid film above the evaporator, and Newton's laws for the motion of the upper diaphragm and evaporator. The model was then linearized for analysis of engine performance. The linear model takes the form

$$\Delta \dot{V}_g + \left[ \frac{(\pi r_i^2)^2}{s_h} + \frac{V_o}{\rho_o R T_o} \right] \Delta \dot{p} - \frac{V_o}{T_o} \Delta \dot{T} = \frac{B}{\rho_o} \Delta T_l - \frac{\beta S}{\rho_o} \sqrt{\frac{M}{2\pi R_u}} \frac{1}{\sqrt{T_o}} \left[ \Delta p - \frac{\rho_o R}{2} \Delta T \right], \quad (1)$$

$$\frac{V_o}{T_o} \Delta \dot{T} - \frac{V_o}{\rho_o c_p T_o} \Delta \dot{p} = -\frac{h_B}{\rho_o c_p T_o} \Delta T, \quad (2)$$

$$\frac{(m + \bar{m})}{(\pi r_o^2)^2} \Delta \dot{V}_g + \frac{(b_f + b)}{(\pi r_o^2)^2} \Delta \dot{V}_g + \frac{s}{(\pi r_o^2)^2} \Delta V_g = \Delta p, \quad (3)$$

$$\frac{C_T}{\rho_o h_{fg}} \Delta \dot{T}_l = \frac{q(t)}{\rho_o h_{fg}} - \frac{U}{\rho_o h_{fg}} \Delta T_l - \frac{B}{\rho_o} \Delta T_l + \frac{\beta S}{\rho_o} \sqrt{\frac{M}{2\pi R_u}} \frac{1}{\sqrt{T_o}} \left[ \Delta p - \frac{\rho_o R}{2} \Delta T \right], \quad (4)$$

where  $\Delta V_g = \pi r_o^2 x$  is the volume change of the vapor bubble caused by motion of the upper membrane;  $\Delta p$ ,  $\Delta T$ , and  $\Delta T_l$  are the departures of vapor pressure temperature, liquid temperature from their ambient values; and  $\bar{\beta}$  is an evaporation coefficient.

Several physically significant parameters appear in these equations. The term  $C_T$  represents thermal storage in the engine. Parasitic heat losses are accounted for by  $U$  and  $h_B$ . It is assumed that an electromechanical energy conversion device can be physically coupled to the upper diaphragm. Its effect is modeled by the damping coefficient  $b$ , while damping  $b_f$  accounts for work lost by friction.

A transfer-function approach was used to analyze the performance of the engine. The heat input  $q(t)$  and diaphragm velocity  $u(t)$  were decomposed into a Fourier series, where  $Q_k$ ,  $U_k$ , were the amplitudes corresponding to  $q(t)$ ,  $u(t)$ ;

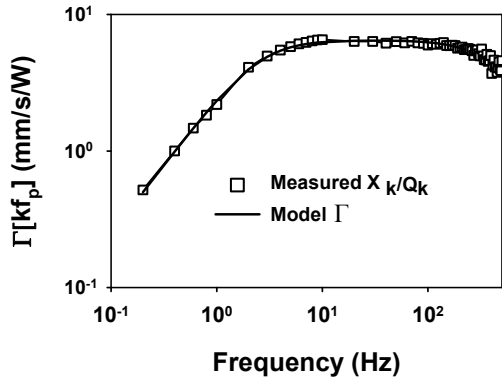


**Fig. 3.** Comparison of model and experimental transfer function.

$T_p=1/f_p$  was the engine cycle period, and  $kf_p$  were the harmonic frequencies. The amplitudes for heat input  $Q_k$  and diaphragm velocity  $U_k$  are related by  $U_k = \Gamma(kf_p) Q_k$ , where  $\Gamma(kf_p)$  is the transfer function magnitude determined from (1-4). The time-averaged power  $\Pi$  generated by the engine was computed with

$$\Pi = \frac{1}{2} \sum_k b |Q_k \Gamma(kf_p)|^2. \quad (5)$$

The time-averaged power  $\Pi$  delivered to the load is proportional to the damping coefficient  $b$ , and the sum-square product  $Q_k \Gamma(kf_p)$ .

### 3. RESULTS AND DISCUSSION

The model was validated by comparison to experimental measurements of the transfer function  $\Gamma(kf_p)$  as shown in Figure 3. Experimental measurements are indicated by the squares while the predictions are shown with a solid line. Experimental values of model parameters such as engine geometry and fluid properties were used in the model. Because estimates of the conduction losses  $h_B$  and  $U$ , thermal storage  $C_T$ , and frictional damping  $b_f$  were not known, these were obtained by minimizing the least square error between model prediction and experimental measurement while holding the fixed parameters constant. Excellent agreement between the model prediction and the experimental data is shown.

The availability of a suitable dynamic model allows extrapolations to explore the influence of

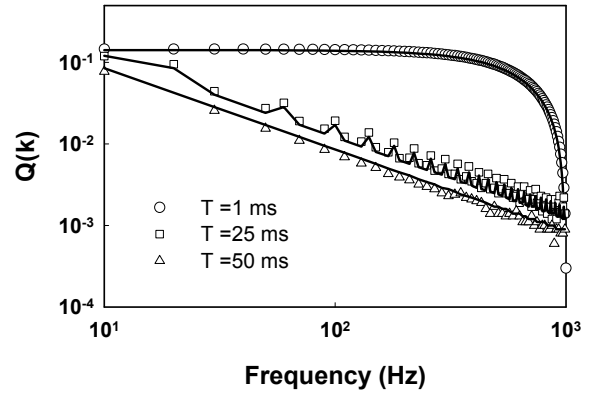


**Fig. 4.** Effect of heat input pulse.

heat rate waveform, thermal storage, energy conversion damping, operational frequency, and engine mass on performance.

Experimental data for heat rate amplitudes  $Q_k$  are shown in Fig. 4. In these experiments, the energy input per cycle remained fixed, the engine cycle frequency was  $f_p=10\text{Hz}$ , and pulse durations of  $T=1, 25$  and  $50\text{ms}$  were used. For pulse durations of  $T=50, 25, 1\text{ms}$ , the amplitudes at  $f_p=10\text{Hz}$  were  $Q_1=0.077, 0.147, 0.147\text{ W}$ . Thus, a heat rate pulse duration less than 10% of the engine cycle period is desirable.

The effect of thermal storage  $C_T$  and energy conversion damping  $b$  on engine performance is shown in Figure 5. Efficiency of the engine was defined as  $\eta=\Pi/ET_p$ , and an operational frequency of  $f_p=100\text{ Hz}$  was used in these computations. As thermal storage  $C_T$  was reduced by a factor of 10, maximum efficiency increased from  $\eta=0.21\%$  to  $\eta=9.43\%$ . It is also apparent that there was an optimal energy conversion coefficient  $b$  with respect to engine efficiency.

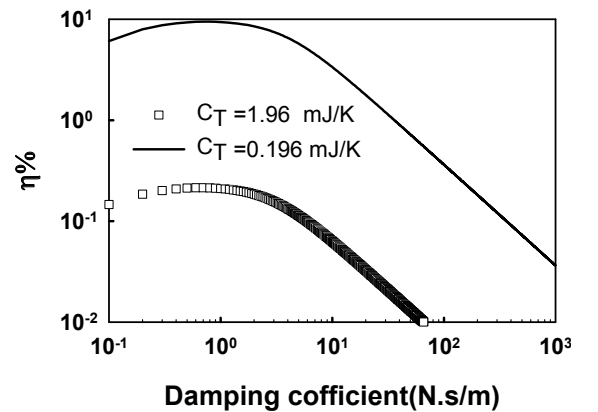


**Fig. 5.** Effect of thermal storage.

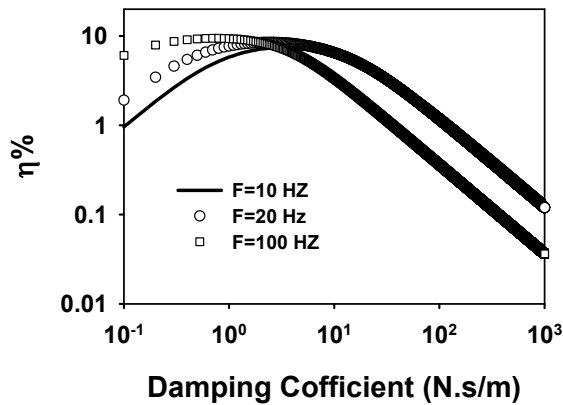


Fig. 6. Effect of damping and frequency.

Consider the plot of engine efficiency versus energy conversion damping  $b$  shown in Figure 6. A thermal storage of  $C_T = 0.196$  mJ/K was used in these computations. Three operational frequencies  $f_p$  were considered. Maximum efficiencies of  $\eta = 7.47\text{--}9.43\%$  were observed at energy conversion damping coefficients  $b$  in the range  $b = 3.4\text{--}0.7$  Ns/m. Higher efficiency was associated with increasing operational frequency  $f_p$ .

Practical choices for electromechanical energy conversion may include piezoelectric, electrostatic, and electromagnetic transduction. In particular, electromagnetic energy conversion will result in an effective damping coefficient of  $b = Bl^2 / (R + R_L)$ , where  $Bl$  is the force coefficient,  $R$  is the coil resistance, and  $R_L$  is a load dissipation resistor modeling an electrical energy storage system. Given values of  $Bl = 1$  N/A,  $R = R_L = 4\Omega$ , a value of  $b = 0.125$  Ns/m is obtained. This value of energy conversion damping coefficient  $b$  is within the range of values suitable for engines considered in the experimental measurements discussed previously.

Finally, consider the effect of resonant operation. Reexamination of Figs. 3-6 reveals no resonant peak of performance. One could conclude that there is no benefit to resonant operation with this configuration. In other words, dissipative effects are large and the quality factor is low. Shown in Fig. 7 are data for an engine with the same geometry and operating conditions but increased mass. At this condition a resonant peak is evident at 250 Hz. Thus, conditions do exist where resonant operation is desirable. The challenge for future work is to use a combination of modeling and experimentation to find the set of design parameters that optimize operation.

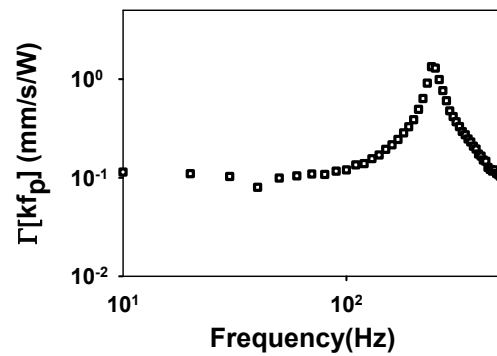


Fig. 7. Effect of added mass.

#### 4. SUMMARY

The dynamic operation of a MEMS heat engine has been studied using a linear transfer function approach. A lumped parameter model was developed and validated with experimental data. The results show that the optimal heat addition pulse is less than 10% of the engine cycle period. Thermal storage in the engine is shown to be detrimental to performance and should be minimized. Conversion of the mechanical work produced by the engine to electrical work by electromagnetic transduction is feasible. Efficiencies on the order of 5 to 10% are predicted for optimal matching of the engine and the load.

#### REFERENCES

1. A. H. Epstein, ASME J. of Eng. For Gas Turbines and Power, Vol. 126, 205 – 226, 2004.
2. K. Fu, A.J., Knobloch, F.C. Martinez, D.C. Walther, C. Fernandez-Pello, A.P. Pisano, D. Leipmann, Proc. ASME IMECE 2001, MEMS-23925, New York, 2001.
3. L.G. Frechette, C. Lee, S. Arslan, Y-C. Liu, Proc. ASME IMECE 2003, Washington DC.
4. J. Cho, L. Weiss, C. Richards, D. Bahr and R. Richards, J. Micromech. Microeng., Vol. 17, p 217 - 223, 2007.
5. L.W. Weiss, J. Cho, K.E. McNeil, D.F. Bahr, C.D. Richards, and R.F. Richards, J. Micromech. Microeng., Vol. 16, p 1-8, 2006.